is better than the presant result, as time approaches to the time limit. For an example, at the $t=20$, the deviation of both results from the exact value are about 2% and 8%, respectively. From the results the Feynman method in the Schlögl model I is more accurate then the star expansion. However, for other systems it can not be said that the solution of the Feynman expansion is better than that of the star expansion, since these two methods have quite different physical meaning as follows: In the Feynman espansion the sources distribute amongst disjointed bundles. Each of them has 2 elements and creates a new source at a subsequent time. This process repeats itsellf with the remaining sources and new ones, until the time t to give a contribution to the solution. However, in star method all the sources gather in a single stage into bundles. These bundles are jointed so that each source can belong to different ones and the resulting contribution to the solution is factorized. It should be mentioned that we may easily obtain an almost exact solution as possible by including the higher other terms in the star expansion, since the star expansion is systematic and simple, as shown in Section (C). Of course, the smaller the ratio $\alpha\xi/\beta$ is, the longer the time region $|b(t)|$ is. In the long time region the linear result deviates from the exact one. This confirms that the multitime scaling method is very useful tool to study nonlinear dynamics.[9,10] The present results in the cases are compared with those obtained by the Feynman method.[8] In the time region where both the approximation are satisfied they agree well each other. For examples the comparisons are shown in Figure 2-6 by choosing $\alpha=0.01$, $\beta=\xi=0.1$, and $\gamma=\omega=1$.

It can be stated that for most cases the linear approximation if quite resonable only in the short time region.[11] Although the present method agrees well with the Feynman method, the former is more systematic and simpler than the latter especially in the multicomponent system.[12] Thus, it may be concluded that the star expansion method is a very powerful tool to discuss the nonlinear phenomena in chemical reaction dynamics.

References

1. C. Itzykson and J. B. Zuber, *Quantum Field Theory* (McGraw-Hill, New York, 1980).
2. F. Schlögl, *Z. Physik*, **253**, 147 (1972).
3. A. Nitzan, P. Ortholeva, J. Deutch, and J. Ross, *J. Chem. Phys.*, **61**, 1058 (1972).
4. J. C. Houard, *Lett. Nuovo Cimento*, **33**, 519 (1982).
5. J. C. Houard and M. Irac-Astaud, *J. Math. Phy.*, **24**, 1997 (1983).
6. J. C. Houard and M. Irac-Astaud, *J. Math. Phy.*, **25**, 3451 (1984).
7. The Dimension of β, γ and ω is time^{-1} and that α and ξ is (concentration time)$^{-1}$. For simplicity the dimensionality is neglected.
8. In the actual comparison the third order expansion terms have been used in both cases.
9. K. O. Han, D. J. Lee, J. M. Lee, K. J. Shin, and S. B. Ko, *Bull. Kor. Chem. Soc.*, **7**, 224 (1986).
10. M. Suzuki, *J. Stat. Phys.*, **16**, 11 (1977).
11. M. H. Ryu, Ph. D. thesis, Chosun University, (1990).
12. In subsequent papers the present method is extend to multicomponent system.

A Theoretical Study of Gas-Surface Phonon Scattering: Model He-Si(100) Bulk and Reconstructed Surfaces

Seung Chul Park*, Chang Hwan Rhee
Woong Lin Hwang†, Yoon Sup Lee†, and Myung Soo Kim‡

Department of Chemistry and Institute of Basic Science, Kangweon National University, Chuncheon 200-701
†Department of Chemistry, Korea Advanced Institute of Science and Technololgy, Seoul 130-650
‡Department of Chemistry, Seoul National University, Seoul 151-742.

Received February 28, 1991

We present a theoretical investigation of the inelastic atom-surface phonon scattering for a model He-Si(100) system by the classical trajectory-quantum forced oscillator(DECENT) method. Single and multi-phonon transition probabilities of normal modes are calculated for several initial beam orientations and several initial kinetic energies. In order to understand surface structure effects, the calculation has been done on both reconstructed and unreconstructed surfaces of the He/Si(100) system. The origin of mode specificity for energy transfer is discussed. The contribution of one, two, and multi-phonon events to the total energy transfer between 0 and 600 K is also given.

Introduction

The study of gas-surface collision dynamics on silicon solid surfaces has become a topic of major interest in surface sciences. There are several reasons for this study. Reactions of gases with the silicon solid surfaces are widely used in micro-fabrications of very-large-scale-intergrated (VLSI) circuits.[1] Energy transfer from atoms and molecules to surface

phonons is fundamental to an understanding of the accommodation coefficient, adsorption and desorption kinetics, as well as the sticking coefficient.[2-4] Collisions between atoms or molecules and the solid surface in the thermal energy range are important in determining the nature of gas-surface interaction potential.[5] These are all important elementary steps in heterogeneous catalysis reactions.

The silicon solid has different reconstructed surfaces depending upon surface symmetries and surface temperatures. The reconstruction of the silicon surfaces has been studied both experimentally[6-9] and theoretically.[10-14] Although effects of electronic structure changes by the surface reconstruction have been studied, the information on dynamic effects of the surface phonons in the gas-surface collision processes is quite limited.[14]

Several model quantum mechanical studies and semiclassical approaches of the atomsurface phonon scattering have been reported.[14-22] Choi and Poe[15,16] have developed the CCTM and the CCRM methods and have applied to resonance and adsorption. Hubbard and Miller[17] used the semiclassical perturbation theory and Billing[18] reported classical energy tranfer into normal modes of a finite surface using a semiclassical method for the CO-Pt(111) system. Several quantum forced oscillator approaches to the gas-surface phonon scattering have been done. Park and Bowman[14] used the DECENT method in a study of single phonon excitations in a He-Si slab system. Smith and Raff[19] have used a wave packet method to the elastic and inelastic atom-surface scattering.

In this paper, we extended the previous work by Park and Bowman[14] on phonon inelastic scattering using the DECENT method to the effects of surface structure changes. We calculated the energy transfer into each phonon mode and the transition probabilities for several initial beam orientations and for several initial collision energies for the reconstructed and unreconstructed (bulk) structures of the silicon surfaces on the phonon scattering. However, the collision energies in this study are limited to low energy regime where phonon energy transfer is significant. We also calculated temperature dependence of the phonon transition probability as well as the contribution of the singel and multiphonon process in the energy transfer on both surfaces. The collision energy dependence of the total energy transfer was also calculated.

In Section II, a brief description of the DECENT method for the gas-surface phonon scattering is presented. Numerical details of the scattering calculations and interaction potentials are described in section III. Results and discussions are given in section IV.

Theory

The approach used here to treat gas-surface collision dynamics is based on the classical trajectory method which has been discussed elsewhere.[14,21-25] The classical trajectory quantum forced oscillator method (DECENT) is based on classical-quantal correspondence of equations of motion for the linearly forced harmonic oscillator which is subject to a time dependent external force.[26-28] This method has been shown to be surprisingly accurate in gas-phase scattering and more accurate than other versions of quantum force oscillator theory.[26] The details of the application of the method have been discussed previously,[14] and we will present only a brief discussion about the key results to be used in the present calculatons.

The main quantity of interest, E_j is the energy transferred into each phonon mode. This (E_j) can be obtained as follows.

$$E_j=\frac{1}{2}\dot{Q}_j^2+\frac{1}{2}\omega_j^2 Q_j^2 \tag{1}$$

where j represents each normal mode and Q_j is the normal coordinate. The ensemble averaged energy transfer, $\langle E_j\rangle$ equals the average of E_j for N trajectories. The energy $\langle E_j\rangle$ can then be directly used in quantum-forced oscillator expression to obtain the transition probability for the j-th phonon to undergo a vibrational transition from i to f *i.e.*[26]

$$P_{i\to f}^{(j)}=|S_{i\to f}^{(j)}|^2=i!\,f!\,e^{\varepsilon_j}\varepsilon_j^{i+f}K_{i\to f}^{(j)2} \tag{2}$$

$$K_{i\to f}^{(j)}=\sum_{l=0}^{\min(i,f)}\frac{(-i)^l\varepsilon_j^{-l}}{(i-l)!\,l!\,(f-l)!} \tag{3}$$

and

$$\varepsilon_j=\frac{\langle E_j\rangle}{\hbar\omega_j} \tag{4}$$

The thermally weighted transition probability for the j-th normal mode at T is

$$W_{i\to f}^{(j)}(T)=O_i^{(j)}(T)\,P_{i\to f}^{(j)} \tag{5}$$

where

$$O_i^{(j)}(T)=\frac{e^{-(i+1/2)\hbar\omega_j/k_BT}}{Q^{(j)}} \tag{6}$$

The multi-mode probability for the transition ($i_1, i_2, \cdots, i_{3N}$) to ($f_1, f_2, \cdots, f_{3N}$) at T is given by

$$W_{(i_1,\,i_2,\,\cdots,\,i_{3N})\to(f_1,\,f_2\,\cdots,\,f_{3N})}=\prod_{j=1}^{3N}W_{i\to f}^{(j)} \tag{7}$$

Thus, the intensity of the one-phonon creation and annihilation of frequency ω_j is given by

$$I(\pm\omega_j;T)=\Big(\sum_i W_{i\to i\pm1}^{(j)}\Big)\prod_{k\neq j}^{3N}\Big(\sum_i W_{i\to i}^{(k)}\Big) \tag{8}$$

And intensities of the overtone and combination bands of two-phonon creation and annihilation are given by

$$I(\pm2\omega_j;T)=\Big(\sum_i W_{i\to i\pm2}^{(j)}\Big)\prod_{k\neq j}^{3N}\Big(\sum_i W_{i\to i}^{(k)}\Big) \tag{9}$$

and

$$I(\pm\omega_j\pm\omega_k;T)=\Big(\sum_i W_{i\to i\pm1}^{(j)}\Big)\Big(\sum W_{i\to i\pm1}^{(k)}\Big)\prod_{l\neq j,\,k}^{3N}\Big(\sum_i W_{i\to i}^{(l)}\Big) \tag{10}$$

respectively.

Calculation

The classical trajectory calculations were performed in the usual manner. As noted, the DECENT method treated the solid atoms initially at their equilibrium positions with no initial velocity. Initial target sites (X, Y) were chosen from an equally spaced grid, 40×40, over the area of the slab and the Z-coordinate was chosen to be normal to the surface.

Table 1. The Normal Mode Frequencies for the Si (100) Bulk and Reconstructed (2×1) Surfaces

Mode number	Bulk $\omega(cm^{-1})$	Reconstructed $\omega(cm^{-1})$	Mode number	Bulk $\omega(cm^{-1})$	Reconstructed $\omega(cm^{-1})$
1	118.17	123.87	43	421.23	423.39
2	118.26	123.89	44	421.58	423.56
3	118.76	123.90	45	421.83	439.82
4	119.66	123.92	46	422.09	441.11
5	126.98	127.50	47	422.17	445.69
6	127.12	127.51	48	422.43	446.82
7	127.14	127.51	49	460.10	460.78
8	127.86	127.53	50	460.11	464.26
9	142.32	138.55	51	460.12	464.49
10	142.91	138.57	52	460.13	464.58
11	146.85	139.58	53	469.58	465.49
12	147.17	140.21	54	469.59	468.09
13	150.51	151.47	55	469.60	469.86
14	151.11	151.48	56	469.61	473.55
15	153.64	154.49	57	501.58	480.36
16	154.12	155.12	58	501.58	481.52
17	155.17	155.13	59	501.58	498.76
18	156.42	157.29	60	504.11	499.07
19	158.70	160.29	61	504.12	499.42
20	161.14	163.95	62	504.14	499.81
21	167.49	224.05	63	504.14	500.08
22	167.71	224.27	64	509.13	500.18
23	173.09	242.95	65	509.13	502.06
24	174.58	243.22	66	509.13	502.14
25	175.32	247.81	67	511.39	503.76
26	175.53	250.13	68	511.40	503.85
27	181.69	263.65	69	511.41	506.45
28	182.73	265.19	70	511.42	506.48
29	240.61	277.28	71	516.57	507.32
30	240.80	277.54	72	516.57	508.15
31	241.06	287.69	73	516.57	539.18
32	241.21	288.24	74	516.85	543.91
33	256.63	361.94	75	516.98	546.06
34	256.94	363.77	76	517.11	550.13
35	257.36	365.87	77	517.17	550.47
36	257.58	367.51	78	517.22	552.18
37	282.44	398.99	79	517.34	554.52
38	282.58	401.37	80	517.48	554.89
39	282.76	410.10	81	517.54	556.20
40	282.85	412.36	82	519.62	558.45
41	420.68	422.53	83	519.62	559.30
42	421.03	422.70	84	519.62	561.31

Thus, 1600 trajectories were calculated under the initial conditions that the collision energy was varied from 150 meV to 900 meV at beam orientation angles, θ of 30°, and ϕ of 0°, 45° and 90°.

The model potential used to describe the interaction of He with Si (100) is the one previously given by Lucchese and Tully.[21] The slab consists of 28 Si atoms for the bilayer, 16 atoms for the first layer and 12 atoms for the second layer. The harmonic interaction between the Si atoms includes the bond stretching force between nearest neighbors, K_R, with the force constants of 1.469 mdyn/A^3 and a harmonic force between second nearest neighbors with a force constant of 0.0890 mdyn/A^3.[21,29] The interaction potential between the He atom and the surface atoms is a pairwise sum of Lennard-Jones 12-6 potentials,

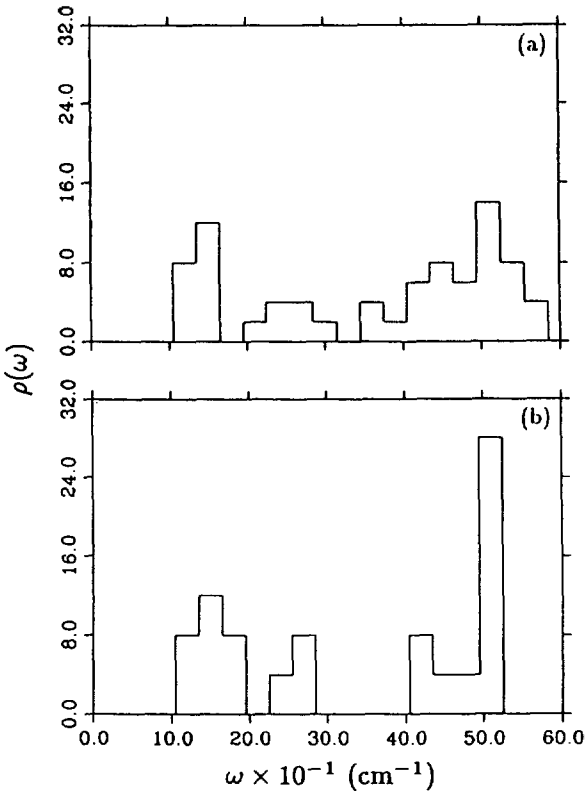

Figure 1. Phonon density of states for the model Si (100) surface, (a) reconstructed (2×1) and (b) unreconstructed (bulk).

$$V(r_0)=\sum_i 4\epsilon\left[\left(\frac{\sigma}{r_{0i}}\right)^{12}-\left(\frac{\sigma}{r_{0i}}\right)^{6}\right] \tag{11}$$

In addition to the pairwise terms, we have also included the contribution from a solid continuum of Lennard-Jones 12-6 potential centers which is of the form,[30]

$$V_S(r)=\frac{2}{3}\pi n_b\sigma^3\epsilon\left[\frac{2}{12}\left(\frac{\sigma}{(z-z_b)}\right)^{9}-\left(\frac{\sigma}{(z-z_b)}\right)^{3}\right] \tag{12}$$

where n_b=0.050 atoms/Å^3 for the number density of Si atoms in the bulk solid and z_b was taken to be half way between the third and fourth planes of the Si atoms.

Results and Discussions

First, we have calculated the 84 normal mode frequencies and eigenvectors for the 28 atom reconstructed Si (100)-(2×1) and unreconstructed Si (100)-bulk harmonic slabs. Table 1 gives these normal mode frequencies. The normal mode frequencies of the reconstructed solid are higher than those of the bulk solid. This is due to the dimer nature of the surface atoms in the reconstructed (2×1) structure which reveals optic mode behavior. We have obtained the density of phonons in a straightforward manner by calculating the number of phonon modes in a given bin of width (30 cm^{-1}),

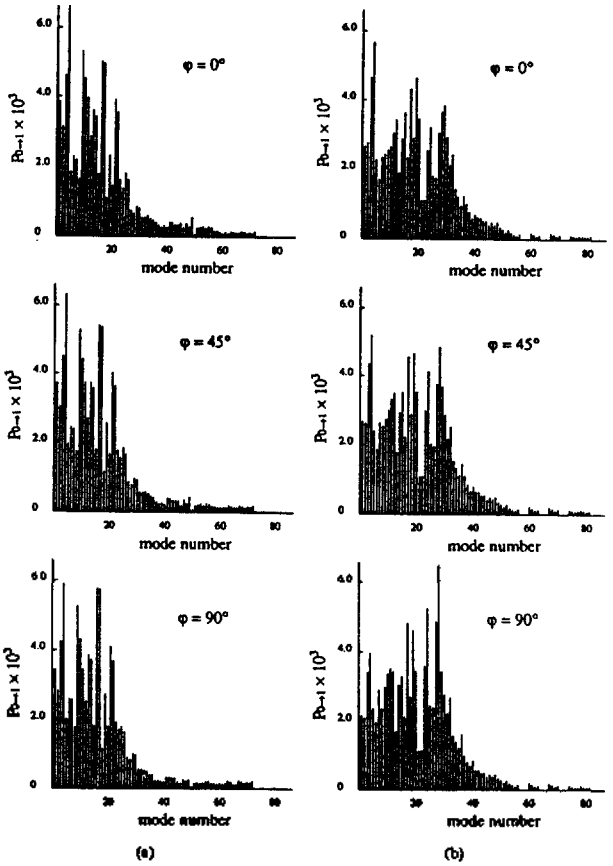

Figure 2. One-phonon transition probabilities versus normal mode number for (a) the reconstructed surface and (b) the bulk structured surface. In all cases, initial kinetic energy is 200 meV and incident angle (θ) is 30°.

and our results are shown in Figure 1. In the lower frequency region, the bulk geometry gives higher density than reconstructed geometry, while in the higher frequency region, the reconstructed geometry gives higher density than the bulk geometry.

In Figure 2, one phonon transition probabilities versus the mode number are plotted for three azimuthal incident angles for the reconstructed and bulk structured Si (100) surface, at the collision energy of 200 meV. In the case of the reconstructed surface, among the modes from 1 to 22, the mode 3, 4, 9, 10, 11, 16, 17, 21, and 22 have relatively high transition probabilities, and the modes 5, 6, 7, 8, 15, 18, 19, and 20 have relatively low transition probabilities. The former are surface localizable modes in character and the latter are similar to the bulk modes projected onto the surface.

The top and the side views of the mode 4 and the mode 16 are drawn in Figure 3. In the mode 4, the surface atom motions are similar to the sagittal plane motion in Rayleigh surface wave,[22] and their effects on the 2nd layer atom motions are reduced. The mode is surface localizable. In the modes 9, 10 and 11, the x-and z-directional motions of the surface atoms are associated similarly to those of the mode 4 with no motions of the subsurface atoms, hence these modes are also the surface localizable modes. In the modes 16 and 17, the surface atoms vibrate in z-direction only, and the 2nd layer atoms vibrate in y-direction in the way that

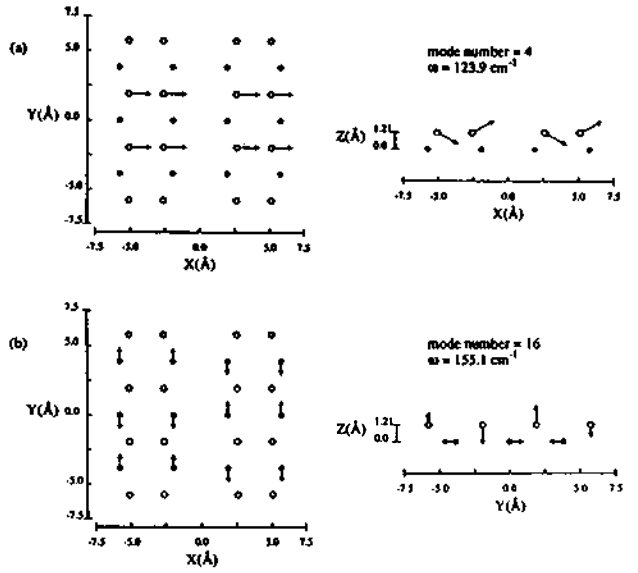

Figure 3. Two normal modes of Si (100)-(2×1) in the xy, xz, or yz plane. Open circles (○) are the first-layer atoms and filled circles(●) are the second-layer atoms.

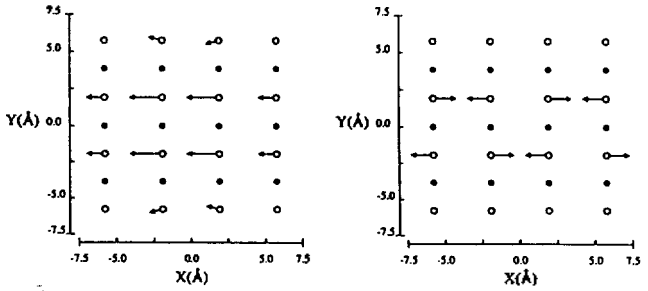

Figure 4. Two normal modes of bulk structured Si (100) surface in the xy plane. Open circles(○) are the first-layer atoms and filled circles(●) are the second-layer atoms.

the repulsive interactions between the surface and the subsurface atoms are reduced as shown in Figure 3. In these modes, the surface atoms have about twice the vibrational amplitudes than the subsurface atoms. Thus, these modes are thought to be the modes decaying into the bulk and surface localization. The modes 5, 6, 7 and 8 have y-directional vibrations of the surface and subsurface atoms with about equal amplitudes and acoustical appearance. These modes are similar to the bulk modes projected onto the surface. The modes 18, 19 and 20 involve x-directional motions of the surface and y-directional motions of the subsurface. These modes are also like the bulk modes rather than the surface modes.

The He atoms are likely to excite mainly the acoustical Rayleigh surface modes,[3] and this affects the mode specificity in the transition probability. Therefore, it follows that He atom is sensitive to the surface modes and is ideal to probe the surface phonon, while neutron is not sensitive to the surface, and phonon is only sensitive to surface waves of very large wavelengths.

As φ changes from 0° to 90°, no significant differences are shown in Figure 2. The transition probability is decreased

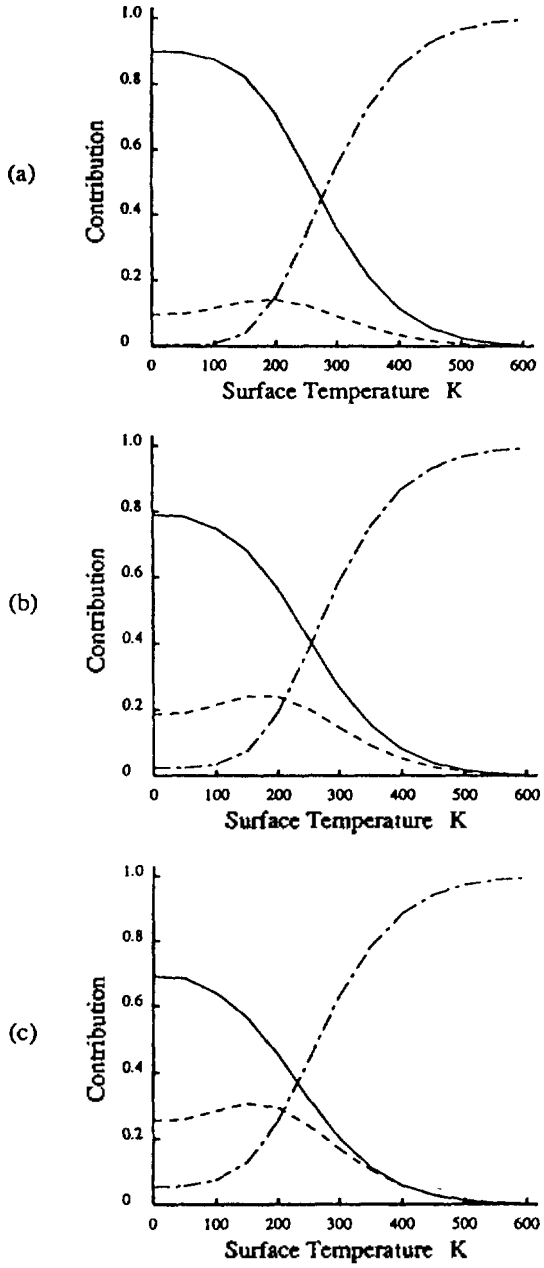

Figure 5. One(——), two(----), and multi-phonon(— —) contributions to the total energy transfer versus surface temperature. Initial kinetic energies of He atom are (a) 200 meV, (b) 400 meV, and (c) 600 meV.

in the mode 4, but increased in the modes 16 and 17. This result is consistent with the expectation that the mode (mode 4) vibrating in x-direction transits less when He atom collides in y-direction ($\phi=90°$) than in x-direction ($\phi=0°$).

In the case of the bulk structured surface, the modes with high transition probabilities have mainly the surface atom motions as in the reconstructed surface. At $\phi=0°$, the mode 4 has the highest transition probability, but at $\phi=90°$, the modes 27 and 28 have, which is not seen in the reconstructed surface. This difference comes from the replacement of the 1st nearest neighbor force constant between the reconstructed dimer with the 2nd nearest neighbor force constant. The dimer whose interaction is strengthened due to reconstruction in Si (100)-(2×1) surface can move freely in the bulk structured surface, but not in the reconstructed surface. The normal modes 4 and 28 of the bulk structured surface are drawn in Figure 4. As in the reconstructed surface, the mode 4, where all surface atoms vibrate in equal phase with the x-directional symmetry, has the highest transition probability at $\phi=0°$. But at $\theta=90°$, the modes 27 and 28, which vibrate with the y-directional symmetry and have no net x-directional momentum, have the highest transition probability. In both cases of reconstructed and bulk structured surfaces, the modes with y-directional surface atom motions have less transition probabilities than the modes with x-directional surface atom motions. The y-directional motions of the surface atoms induce the 2nd layer atom motions.[14] This fact indicates that He atom collision process is sensitive to the surface atom motion.[3]

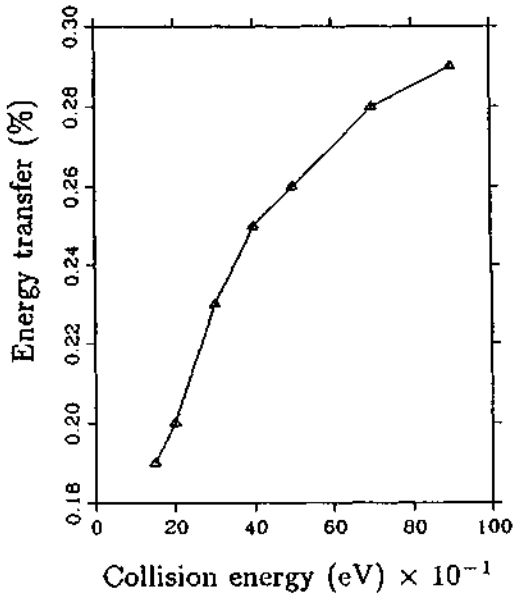

Figure 6. Percent of energy transfer into phonons versus incident kinetic energies.

Figure 5 represents the temperature dependence of one, two and multi-phonon contributions to the total energy transfer. In this system the one phonon contribution is a major part of the energy transfer at low temperatures, but at high temperatures, the multi-phonon contribution is dominant. In two and multi-phonon transitions, as temperature goes up, the possible number of cases for the processes increases tremendously. Once excited vibrational states are populated, the cases for the multi-phonon processes which include one phonon creations and annihilations and two phonon overtones, and combinations of them, etc. increase enormously. Therefore, even though each process in the two phonon transitions has about three orders of magnitude smaller probability than the one phonon process, the multi-phonon transitions occur predominantly at high temperature. Near the zero temperature, all modes exist significantly in their ground state, thus, the one phonon transitions occur significantly.

We have also calculated the energy transferred to the surface at incident kinetic energies of 150, 200, 300, 400, 500, 700 and 900 meV, and we have obtained the energy transferred per incident kinetic energy to be 0.19, 0.20, 0.23, 0.25,

0.26 0.28 and 0.29 respectively, which is shown in Figure 6. The energy transferred into phonons increases as the incident collision energy is increased. In the low lenergy region, *i.e.*, less than 400 meV, the rate of energy transfer sharply increases while in the high energy region, the rate is reduced.

Acknowledgment. This work was supported in part by the Korea Research Foundation, Ministry of Education (1987) and by the Basic Science Research Institute Program, Ministry of Education (BSRI-90-301).

References

1. C. J. Mogab, *in VLSI Technology*, edited by S. M. Sze (McGraw-Hill, New York, 1983) Chapter 8, 303-346.
2. J. C. Tully, *Ann. Rev. Phys. Chem.*, **31**, 319 (1980).
3. J. P. Toennies, *in Dynamics of Gas-Surface Interaction*, edited by G. Benedek and U. Valbusa (Springer, Berlin, 1982) pp. 208-226.
4. G. A. Somorjai, *Chemistry in Two Dimensions: Surface* (Cornell University, New York, 1981), Chapter 7, pp. 331-380.
5. D. Eichenauer and J. P. Toennies, *J. Chem. Phys.*, **85**, 532 (1986).
6. J. J. Lander and J. Morrison, *J. Chem. Phys.*, **37**, 729 (1962).
7. E. T. Gawlinski and J. D. Guton, Phys. Rev., **B36**, 4774 (1987).
8. F. F. Abraham and J. Q. Broughton, *Phys. Rev. Lett.*, **56**, 734 (1986).
9. R. J. Hamers, R. M. Tromp, and J. E. Demuth, *Phys. Rev.*, **B34**, 5347 (1986).
10. R. A. Stansfield, K. Broomfield, and D. C. Clary, *Phys. Rev.*, **B39**, 7680 (1989).
11. R. Biwas and D. R. Hamann, *Phys. Rev. Lett.*, **55**, 2001 (1985).
12. R. Lampinen, R. M. Nieminen, and K. Kasaki, *Surf. Sci.*, **203**, 201 (1988).
13. F. F. Abraham and I. P. Batra, *Surf. Sci.*, **163**, L752 (1985).
14. S. C. Park and J. M. Bowman, *J. Chem. Phys.*, **81**, 6277 (1984).
15. B. C. Choi and R. T. Poe, *J. Chem. Phys.*, **83**, 1330 (1985).
16. B. C. Choi and R. T. Poe, *J. Chem. Phys.*, **83**, 1334 (1985).
17. L. M. Hubbard and W. H. Miller, *J. Chem. Phys.*, **80**, 5827 (1984).
18. G. D. Billing, *Chem. Phys.*, **86**, 349 (1984).
19. C. B. Smith and L. M. Raff, *J. Chem. Phys.*, **83**, 1411 (1985).
20. H.-D. Meyer, *Surf. Sci.*, **104**, 117 (1981).
21. R. R. Lucchese and J. C. Tully, *Surf. Sci.*, **137**, 570 (1984).
22. R. R. Lucchese and J. C. Tully, *J. Chem. Phys.*, **80**, 3451 (1984).
23. S. C. Park and D. C. Clary, *J. Appl. Phys.*, **60**, 1183 (1986).
24. S. C. Park and J. M. Bowman, *J. Chem. Phys.*, **80**, 3845 (1984).
25. S. A. Adelman and J. M. Doll, *J. Chem. Phys.*, **61**, 4242 (1974).
26. W. R. Gentry and C. F. Giese, *J. Chem. Phys.*, **63**, 3144 (1975).
27. H.-D. Meyer, *Chem. Phys.*, **61**, 365 (1981).
28. R. P. Feynman and A. R. Hibbs, *Quantum Mechanics and Path Integrals* (McGrawHill, New York, 1965), Chapter 8, pp. 232-234.
29. R. Tubino, L. Piseri, and G. Zerbi, *J. Chem. Phys.* **56**, 1022 (1972).
30. W. A. Steele, *The Interaction of Gases with Solid Surfaces* (Pergamon, Oxford, 1974).

Formal Synthesis of Isocomene

Hyo Won Lee*

**Jae Hyun Lee and Ihl-Young Choi Lee*

Korea Research Institute of Chemical Technology, Daejeon 302-343. *Received March 6, 1991*

A stereocontrolled synthesis of (±)-isocomene (**1**) *via* selective monoketalization of tricyclo[6.3.0.0^{1,5}]undeca-4,7-dione (**13**) was reported. Grignard reaction of bicyclic enone **10**, which was prepared from 2-methyl-1,3-cyclopentadione, gave the 1,4-addition product **11**. The subsequent aldol condensation product **12** was converted to mesyl derivative **13**. Transformation from **13** to the desired product **19** was achieved by a series of reactions, *i.e.*, the selective monoketalization at C-4 carbonyl group, the elimination of a mesyl group, Birch alkylation, methylation at C-6, the reduction of carbonyl group, the dehydration of alcohol **18**, and hydrolysis of the ketal group.

Introduction

The tricyclic sesquiterpene isocomene (**1**) has the unique framework of tricyclo[6.3.0.0^{1,5}]undeca-4,7-dione which comprises a variety of the polyquinanes. Since the first isolation of the tricyclic sesquiterpene isocomeme (**1**) in 1977 from